Chemical Science

EDGE ARTICLE

View Article Online
View Journal | View Issue

Cite this: *Chem. Sci.*, 2016, **7**, 499

A NIR dye with high-performance n-type semiconducting properties†

Jiajun Xie, Ke Shi, Kang Cai, Di Zhang, Jie-Yu Wang, Jian Pei* and Dahui Zhao*

Received 17th August 2015
Accepted 5th October 2015

DOI: 10.1039/c5sc03045e

www.rsc.org/chemicalscience

A novel hetero-polycyclic aromatic compound manifesting strong near-infrared (NIR) absorption as well as high-performance n-type semiconducting properties is developed. With an exceptionally low LUMO level at −4.7 eV, this NIR dye ($\lambda_{max} \approx 1100$ nm, $\varepsilon \approx 10^5$ mol^{-1} L cm^{-1}) exhibits adequate stability under ambient conditions, with electron mobility up to 0.96 cm^2 V^{-1} s^{-1} measured in solution-processed organic field-effect transistors. A special metal-free C–C coupling serves as a pivotal step in constructing the polycyclic π-framework of this low-bandgap chromophore, by fusing an electron-deficient naphthalenediimide moiety with an electron-donating naphthalenediamine. Such a rare combination of extraordinary optical and semiconductive attributes is quite valuable for organic small molecules, and promising for unique applications in the opto-electronic field.

Introduction

Organic molecules with pronounced near-infrared (NIR) absorptions are valuable optical, opto-electronic, and bio-applicable materials.[1–3] However, in spite of all the efforts made to acquire the low-bandgap feature, up to now only a limited number of air-stable closed-shell, neutral organic small molecules have been developed possessing optimal NIR optical activity. Moreover, their absorptions mostly fall in the range of 700–900 nm. Very few neutral organic small molecules possess a desirable extinction ability beyond 1000 nm.[4,5] The challenges in designing potent NIR dyes lie in the fact that, in order to attain a low-energy bandgap with a significant extinction coefficient, fine tuning the ground and excited electronic states is required to achieve not only suitable energy levels but also an adequate transition dipole moment. Particular care should also be taken to avoid a detrimental effect on the chemo-stability, which could result from over-boosting the HOMO or over-depressing the LUMO.

A common strategy to attain a low-energy bandgap in an organic structure relies on incorporating electron donator (D) and acceptor (A) moieties into the same molecule, preferably linked by a π-conjugated spacer to extend the effective conjugation length.[6] However, in many cases separately installed D and A subunits impart a very limited extinction coefficient to the low-energy excited state. Also, the charge transfer nature may render the optical behavior highly sensitive to environmental polarity variation.[7]

Another effective approach to developing low-bandgap chromophores utilizes large polycyclic π-systems.[8] A major advantage of polycyclic aromatic compounds is their readily tuned HOMO/LUMO energy levels. Through chemical modifications, D/A substituents can also be incorporated. Moreover, large π-systems with delocalized frontier orbitals also promote enhanced light-absorbing ability. Previously, we developed a number of *N*-hetero-polycyclic dicarboximide molecules manifesting absorptions around 800–900 nm.[9] The syntheses of these molecules harnessed 2,3,6,7-tetrabromo-1,4,5,8- tetracarboxydiimide (**4Br-NDI**) as an important synthon.[10] The highly electron-deficient NDI allows exploitation of facile nucleophilic substitution reactions to functionalize and expand the polycyclic π-skeleton. Moreover, the strongly electron-pulling dicarboximide groups help confer an adequately low LUMO to the designed products, favorable for inducing NIR optics. In these previous designs, benzene-1,2-diamine and 1,2,4,5-tetramine were applied to react with **4Br-NDI** *via* their *N*-nucleophilic sites. Thus, polycyclic products were formed featuring both electron-accepting NDI and electron-rich dihydrophenazine moieties, bringing about the NIR-absorbing attributes.

In the current work, we integrate naphthalene-1,5-diamine with two equivalents of **4Br-NDI** to construct a polycyclic NIR chromophore, *via* a tandem reaction entailing a nucleophilic aromatic substitution (S_NAr) followed by a unique metal-free C–C coupling. A large *N*-hetero-polycyclic tetraimide molecule **1** (Scheme 1) exhibiting absorptions at *ca.* 1000 nm was thus obtained. Upon further functionalizing with 2-(dimercaptomethylene)malononitrile, molecule **2** was achieved, impressively manifesting major absorption around 1100 nm ($\varepsilon > 10^5$ mol^{-1} L cm^{-1}). Besides the

Beijing National Laboratory for Molecular Sciences, Centre of Soft Matter Science and Engineering, Key Lab of Polymer Chemistry & Physics of Ministry of Education, College of Chemistry, Peking University, China. E-mail: dhzhao@pku.edu.cn; jianpei@pku.edu.cn

† Electronic supplementary information (ESI) available: Syntheses, characterization data, and DFT calculations. See DOI: 10.1039/c5sc03045e

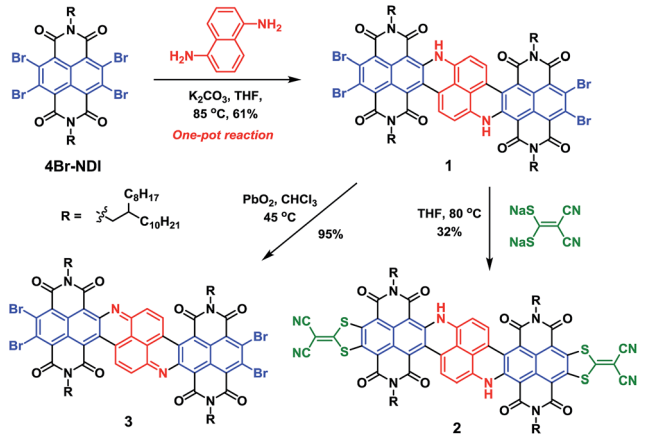

Scheme 1 Synthetic route.

very narrow optical bandgap, compound **2** also possessed an exceptionally low LUMO level at −4.72 eV. Such a low LUMO level greatly favoured the electron-transporting ability. A remarkable electron mobility up to 0.96 $cm^2 V^{-1} s^{-1}$ was determined for **2** in a solution-processed thin-film transistor. The notable stability of **2** was underscored by comparison to molecule **3** with a similarly low LUMO level. Such a rare combination of high stability, strong NIR absorption, and optimal n-type semiconducting performance endows molecule **2** with great potential for opto-electronic applications.

Results and discussion

By subjecting naphthalene-1,5-diamine to excess **4Br-NDI**, we were initially expecting a double S_NAr product **1a**′ (Scheme S1†), which was then planned to be transformed to **1** under separate Heck-coupling conditions. However, after working up the reaction of naphthalenediamine and **4Br-NDI** in the presence of K_2CO_3, the ^1H NMR spectrum indicated that two aromatic protons were missing from the expected **1a**′. The mass spectroscopy also revealed that, while the generated molecule incorporated two NDI units, it contained only four bromine atoms. After analyzing the complete characterization results, we concluded that molecule **1** was produced in one pot from naphthalene-1,5-diamine and **4Br-NDI** in the absence of the Pd catalyst (Scheme 1).

The mechanism of this tandem process was then examined in more detail. Molecule **4** was obtainable in decent yield at a shortened reaction time and lowered temperature, while **4a** was not isolated. Since **4Br-NDI** was known to undergo substitutions with various nucleophiles,[10] S_NAr between **4Br-NDI** and naphthalenediamine reasonably happened (Scheme 2). Since debromination was not detected with **4a** or **1a**, the following intramolecular C–C coupling was unlikely to involve redox processes.[11] Moreover, it was found that molecule **1** was formed much faster in tetrahydrofuran than toluene, with nearly identical yields, which also suggested a polar mechanism. We thus proposed that the intramolecular C–C coupling was a S_NAr process for the bromo-NDI moiety, with $C(sp^2)H$ as the nucleophile (Scheme 2). It was suspected that the strongly electron-donating NH was a critical activator in this electrophilic aromatic substitution of naphthalenediamine, by conferring high nucleophilicity to its *para*-position. To prove this hypothesis, we then carried out a reaction between **4Br-NDI** and 1,3-phenylenediamine. As expected, molecule **5** was generated, substantiating the notion that NH activated its *para*-CH and realized a 5-membered ring annulation (Schemes 2 and S2†).

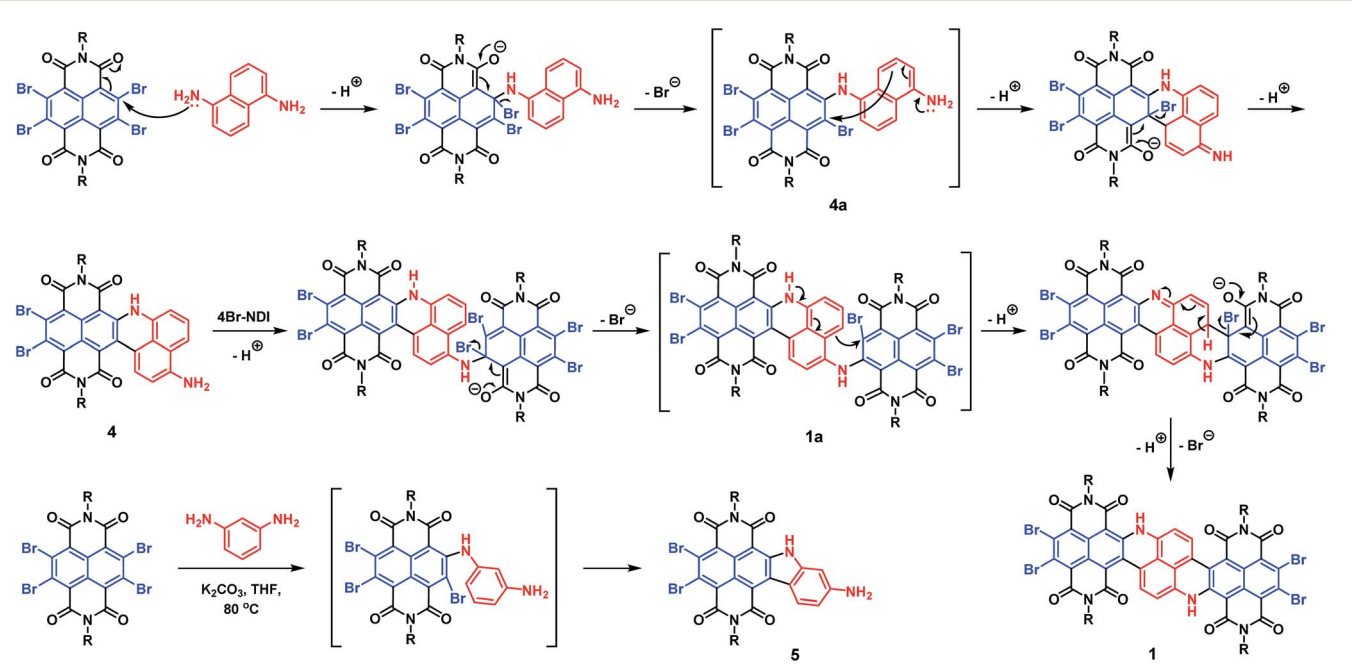

Scheme 2 Proposed reaction pathways to **1** and **5**.

The UV/vis/NIR absorption spectrum of **1** showed a broad absorption band in the range of 600–1200 nm (Fig. 1a), and the maximum (λ_{max}) emerged at *ca.* 1000 nm, with a large molar extinction coefficient (ε) of 1.2×10^5 L mol^{-1} cm^{-1}. The vibronic structures were clearly observable, consistent with the highly rigid polycyclic skeleton of the chromophore.[5,12,13]

Impressed by the remarkable NIR optical properties of **1**, we were intrigued to investigate whether the bandgap could be further narrowed through chemical modifications. After various attempts, molecule **2** was successfully prepared by subjecting compound **1** to sodium 1,1-dicyanoethylene-2,2-dithiolate. Such a modification was anticipated to further lower the bandgap since the resultant **2** possessed a further expanded polycyclic π-system with more intense D–A characteristics. Desirable results were observed when the absorption spectrum of **2** was collected. While the band shape remained quite similar to that of **1**, the overall spectrum was shifted to a longer wavelength by about 100 nm, giving rise to λ_{max} at *ca.* 1100 nm with $\varepsilon > 1.3 \times 10^5$ L mol^{-1} cm^{-1} (Fig. 1a). Such strong absorptions around 1100 nm are observed for the first time with closed-shell polycyclic dicarboximide dye molecules.

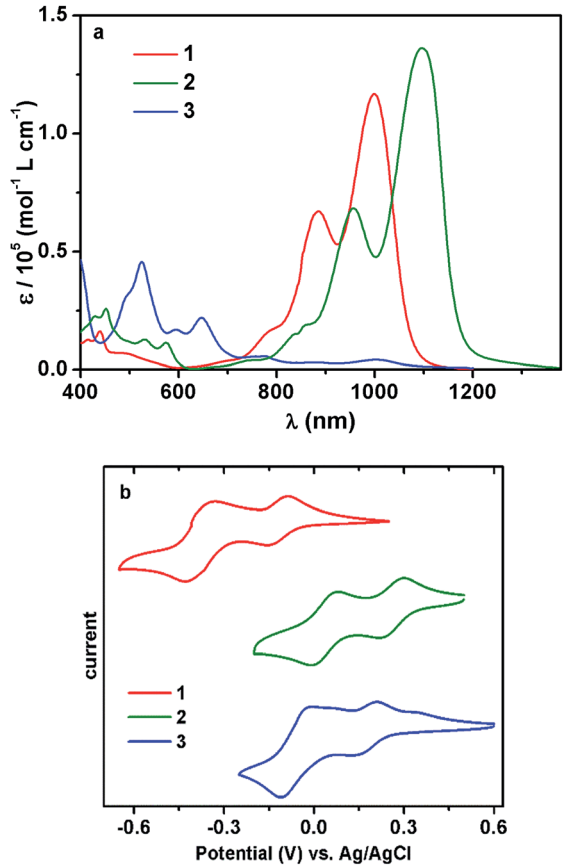

Fig. 1 (a) UV-vis-NIR absorption spectra (at 1.0×10^{-5} M in $CHCl_3$); (b) cyclic voltammograms of **1–3** recorded in $CHCl_3$.

The absorption spectra of **1** and **2** at varied concentrations suggested that these molecules were weakly aggregating in chloroform (Fig. S1 and S2†). Both **1** and **2** were weakly luminescent, exhibiting small Stokes shifts of 412 and 257 cm^{-1}, respectively (Fig. S4 and S5†).

Subsequent electrochemical study unveiled that the much narrowed bandgap of **2** was mainly attributable to its substantially lowered LUMO level. As shown by the cyclic voltammograms (CV), both **1** and **2** displayed two reduction and two oxidation waves (Fig. 1b and S8†). All these redox processes were reversible. A particularly low LUMO at −4.72 eV was displayed by **2**, in comparison to the LUMO at −4.35 eV for **1** (Table 1). On the other hand, the HOMO energy levels of the two molecules were separated by 0.03 eV, which explained the much narrower bandgap of **2**. It is noteworthy that, in spite of such a low-lying LUMO and narrow bandgap, compound **2** was fairly stable under ambient conditions. No detectable changes were observed in the absorption or NMR spectra after storing under ambient conditions for months.

The remarkable stability of **2** was further underlined by comparison to molecule **3** with a similarly low LUMO. Compound **1** could be oxidized to **3** in nearly quantitative yield using PbO_2 (Scheme 1). This redox process was well reversible, and the reduction of **3** back to **1** was realized, also quantitatively, with 1,4-phenylenediamine. The absorption spectrum showed that molecule **3** also possessed a low-energy $S_0 \rightarrow S_1$ band in the NIR regime, exhibiting a local maximum at about 1000 nm, but this low-energy transition displayed minimal extinction ability (Fig. 1a). The overall absorption maximum at a much higher energy emerged around 525 nm. Not surprisingly, CV revealed that the dehydrogenated molecule **3** displayed a considerably lowered LUMO at −4.66 eV compared to **1**, actually slightly higher than that of **2** (Table 1). However, unlike compound **2**, inferior chemo-stability was observed with **3**. Both absorption and NMR spectra indicated that molecule **3** was partially reduced to **1** after storing under ambient conditions for only a few days. The similar LUMO level but superior

Table 1 Optical and electronic properties

	λ_{abs}[a] [nm]	ε[b] [mol^{-1} L cm^{-1}]	λ_{em}[c] [nm]	LUMO[d] [eV]	HOMO [eV]	LUMO–HOMO[d] [eV]	E_g[e] [eV]
1	1000	1.2×10^5	1043	−4.35	−5.27[d]	0.92	1.09
2	1101	1.4×10^5	1133	−4.72	−5.30[d]	0.58	0.99
3	1004	4.7×10^3	—	−4.66	−5.80[f]	—	1.14

[a] Absorption maxima of the $S_0 \rightarrow S_1$ transition in $CHCl_3$ solution. [b] Molar extinction coefficient at λ_{abs}. [c] Emission maxima in $CHCl_3$. [d] Data from CV. [e] Optical bandgap from the absorption onset. [f] Calculated from the optical bandgap and LUMO in CV.

chemo-stability of **2** compared to **3**, by virtue of the dihydro-structure, further stressed the precious values of the former.

Time-dependent density functional theory (TD-DFT) calculation results confirmed the experimental observations by showing that the $S_0 \rightarrow S_1$ transition in compound **3**, corresponding to electron excitation from HOMO to LUMO, possessed a much smaller oscillator strength compared to its higher energy transitions (Fig. S14†). DFT and TD-DFT calculations were also performed for **1** and **2**. Remarkably, the HOMO and LUMO of **1** and **2** were extensively delocalized over the entire polycyclic π-framework (Fig. 2). Consistent with the experimentally observed strong NIR absorbing abilities of **1** and **2**, TD-DFT calculations also verified that both molecules manifested very large transition dipole moments and significant oscillator strengths with their low-energy $S_0 \rightarrow S_1$ (HOMO to LUMO) transitions.

The low-lying LUMO level and delocalized frontier orbitals[14] of **2** prompted us to examine its electron-transporting semiconducting capability.[15] To this end, organic field-effect transistors (OFET) with top-gate/bottom-contact configuration were fabricated. Using the solution processing technique, the active layer was deposited by spin-casting solutions of **2** in trichloroethylene (10 mg mL^{-1}) on patterned Au(source–drain)/SiO_2/Si substrates. After thermal annealing the semiconducting materials, a poly(perflurobutenylvinylether) (CYTOP) solution was spin-coated on top of it as the dielectric layer, followed by thermally evaporating a layer of aluminum as the gate electrode. All devices were fabricated in a glove box but tested under ambient conditions (R_H = 50–60%). As expected, molecule **2** exhibited typical n-type transport characteristics. Quite impressively, optimal electron mobility (μ_e) up to 0.96 $cm^2\ V^{-1}\ s^{-1}$ (Fig. 3) and an average μ_e of 0.93 $cm^2\ V^{-1}\ s^{-1}$ were determined. In comparison, an electron mobility of merely 0.007 $cm^2\ V^{-1}\ s^{-1}$ (Fig. S11†) was measured for **1** under similar conditions, while compound **3** was not completely stable (partially reduced) during the device fabrication.

Notably, the transfer and output characteristics of **2** showed negligible hysteresis, which has rarely been observed for n-type organic materials and could be attributable to the low LUMO of the molecule. Besides, no contact resistance was observed in the output curves, suggesting good contact between molecule **2** and the gold electrode.

In the device characterizations, it was noticed that the electron mobility of **2** was highly sensitive to the annealing temperature (Fig. S10†). TGA and DSC characterizations confirmed adequate thermal stability of molecule **2** (Fig. S9†), so a relatively wide range of annealing temperatures was examined. When the semiconductor was annealed at 100 °C, only a moderate electron mobility of 0.12 $cm^2\ V^{-1}\ s^{-1}$ was obtained. Whereas, if the annealing temperature was elevated to 150 °C, the electron mobility was significantly improved to 0.73 $cm^2\ V^{-1}\ s^{-1}$. More desirable performances were achieved between 180 and 250 °C, with the mobility fluctuating in the range of 0.8–1.0 $cm^2\ V^{-1}\ s^{-1}$ (Fig. S10†). Moreover, at the optimized annealing temperature, very low V_{Th} values of −5 to 0 V were observed. Subsequently, AFM and X-ray diffraction studies elucidated that the variation in the device performance was clearly correlated to the crystallinity of the semiconducting

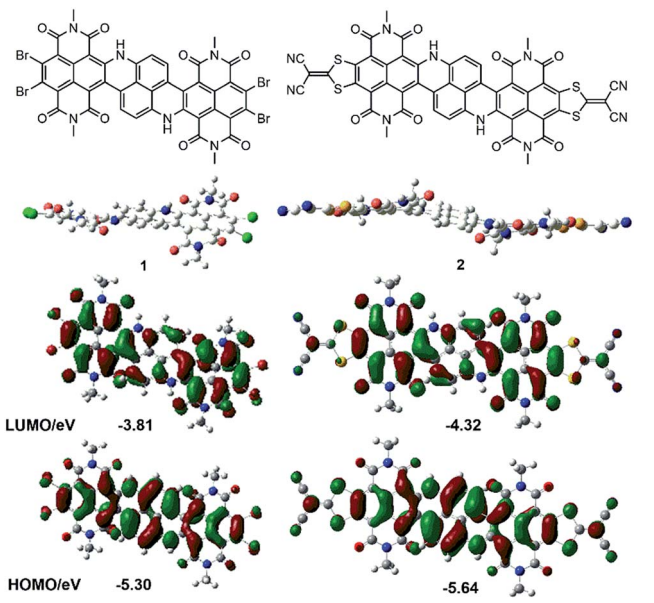

Fig. 2 DFT calculated geometry (side view) and HOMO/LUMO (top view) of **1** and **2** (alkyl side groups are replaced by methyl in the calculations).

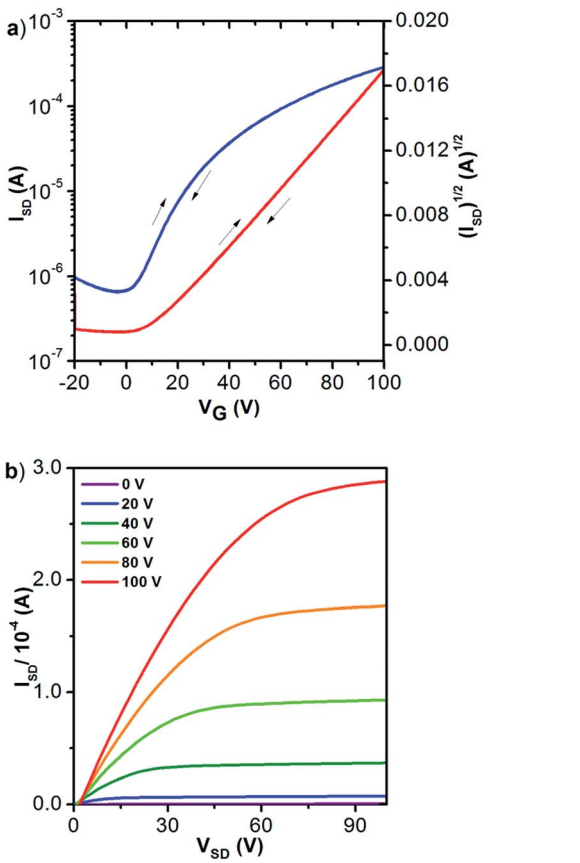

Fig. 3 (a) Transfer (V_{DS} = 100 V) and (b) output profiles of **2** (annealed at 220 °C) in OFET (μ_e = 0.96 $cm^2\ V^{-1}\ s^{-1}$).

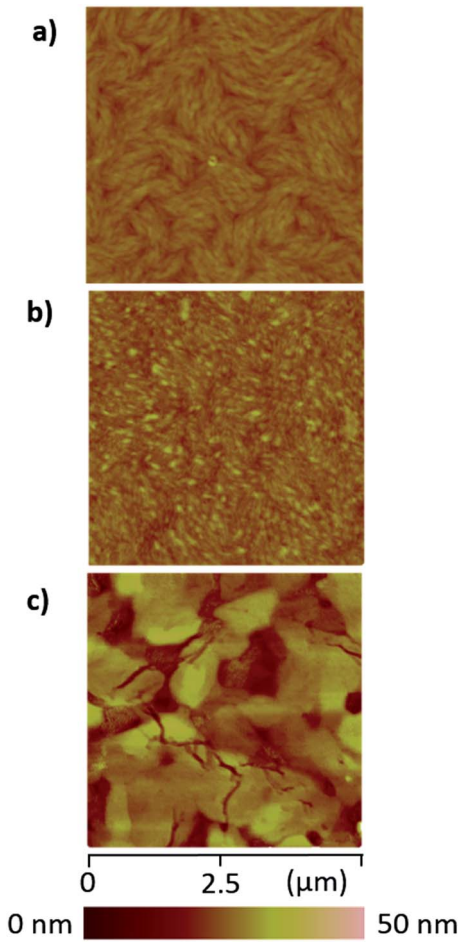

Fig. 4 AFM height images of thin films of **2** upon thermal annealing at (a) 100 °C, (b) 180 °C and (c) 220 °C.

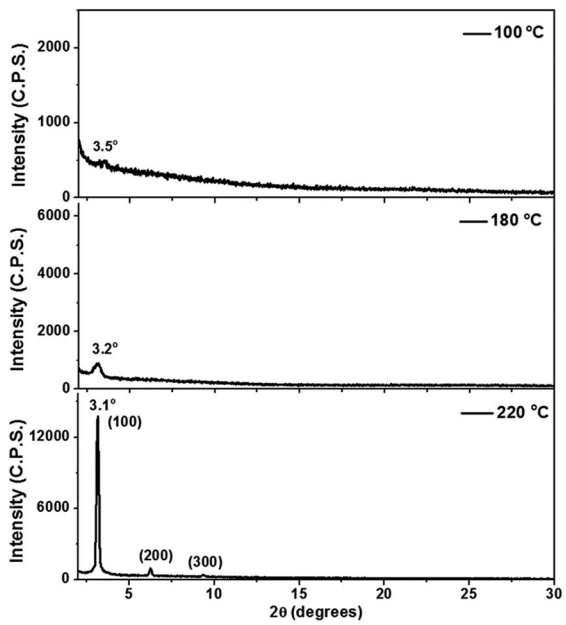

Fig. 5 XRD profiles of thin films of **2** after thermal annealing at varied temperatures.

layer. Highly crystalline morphology and best device performance were both obtained after annealing at about 220 °C (Fig. 4 and 5). Such high electron mobility, as well as the low V_{Th} value, is believed to benefit from the low-lying LUMO and suitable frontier orbital distribution of **2**. The S···S interactions may have helped to induce a favorable molecular packing motif.

Conclusions

In conclusion, a neutral organic small molecule **2** exhibiting strong NIR absorption around 1100 nm ($\varepsilon \approx 10^5$ mol^{-1} L cm^{-1}) and an electron mobility up to 0.96 cm^2 V^{-1} s^{-1} is developed. The synthesis of the molecule is accomplished *via* a tandem process, involving a unique metal-free C–C coupling reaction between an electrophilic aryl bromide and an electron-rich aryl amine with dual nucleophilic sites of NH and CH groups. Having an exceptionally low-lying LUMO at −4.72 eV, the advantageously high chemo-stability of **2** is highlighted by comparison to molecule **3**, which has a slightly higher LUMO than **2** but undergoes auto-reduction under ambient conditions. Such a combination of low-energy NIR-absorption, n-type semiconducting ability and optimal chemo-stability is rarely available for organic molecules. To the best of our knowledge, this is the first example of an organic small molecule that manifests both high performance n-type semiconducting properties and strong NIR absorption at wavelengths exceeding 1 μm. Such distinctive properties qualify the molecule for special applications as a transparent organic opto-electronic material.

Acknowledgements

We acknowledge the financial support from the National Natural Science Foundation (No. 21174004, 21222403 and 51473003).

Notes and references

1 (*a*) S. Baluschev, V. Yakutkin, T. Miteva, Y. Avlasevich, S. Chernov, S. Aleshchenkov, G. Nelles, A. Cheprakov, A. Yasuda, K. Müllen and G. Wegner, *Angew. Chem., Int. Ed.*, 2007, **46**, 7693; (*b*) G. Qian, Z. Zhong, M. Luo, D. Yu, Z. Zhang, Z. Y. Wang and D. Ma, *Adv. Mater.*, 2009, **21**, 111; (*c*) R. E. Dawson, A. Hennig, D. P. Weimann, D. Emery, V. Ravikumar, J. Montenegro, T. Takeuchi, S. Gabutti, M. Mayor, J. Mareda, C. A. S. Challey and S. Matile, *Nat. Chem.*, 2010, **2**, 533.

2 (*a*) U. Mayerhöffer, K. Deing, K. Gruβ, H. Braunschweig, K. Meerholz and F. Würthner, *Angew. Chem., Int. Ed.*, 2009, **48**, 8776; (*b*) M. Liang and J. Chen, *Chem. Soc. Rev.*, 2013, **42**, 3453; (*c*) L. L. Li and E. W. G. Diau, *Chem. Soc. Rev.*, 2013, **42**, 291; (*d*) L. Yao, S. Zhang, R. Wang, W. Li, F. Shen, B. Yang and Y. Ma, *Angew. Chem., Int. Ed.*, 2014, **53**, 2119.

3 (*a*) Y. Wang, D. Gao, P. Zhang, P. Gong, C. Chen, G. Gao and L. Cai, *Chem. Commun.*, 2014, **50**, 811; (*b*) A. P. Jathoul, H. Grounds, J. C. Anderson and M. A. Pule, *Angew. Chem.,*

Int. Ed., 2014, **53**, 13059; (*c*) M. Li, X. Wu, T. Wang, Y. Li, W. Zhu and T. D. James, *Chem. Commun.*, 2014, **50**, 1751; (*d*) X. Wu, X. Sun, Z. Guo, J. Tang, Y. Shen, T. James, H. Tian and W. Zhu, *J. Am. Chem. Soc.*, 2014, **136**, 3579.

4 (*a*) G. Qian, B. Dai, M. Luo, D. Yu, J. Zhan, Z. Zhang, D. Ma and Z. Wang, *Chem. Mater.*, 2008, **20**, 6208; (*b*) G. Qian and Z. Wang, *Can. J. Chem.*, 2010, **88**, 192; (*c*) G. Qian and Z. Wang, *Chem.–Asian J.*, 2010, **5**, 1006.

5 (*a*) C. Kohl, S. Becker and K. Müllen, *Chem. Commun.*, 2002, 2778; (*b*) V. J. Pansare, S. Hejazi, W. J. Faenza and R. K. Prudhomme, *Chem. Mater.*, 2012, **24**, 812.

6 (*a*) J. Fabian, H. Nakazumi and M. Matsuoka, *Chem. Rev.*, 1992, **92**, 1197; (*b*) N. Sakai, J. Mareda, E. Vauthey and S. Matile, *Chem. Commun.*, 2010, **46**, 4225; (*c*) Y. Matsunaga, K. Goto, K. Kubono, K. Sako and T. Shinmyozu, *Chem.–Eur. J.*, 2014, **20**, 7309.

7 Z. Guo, Z. Jin, J. Wang and J. Pei, *Chem. Commun.*, 2014, **50**, 6088.

8 (*a*) J. E. Anthony, *Angew. Chem., Int. Ed.*, 2008, **47**, 452; (*b*) W. Yue, J. Gao, W. Jiang, S. Motta, F. Negri and Z. Wang, *J. Am. Chem. Soc.*, 2011, **133**, 18054; (*c*) L. Chen, C. Li and K. Müllen, *J. Mater. Chem. C*, 2014, **2**, 1938.

9 (*a*) K. Cai, Q. Yan and D. Zhao, *Chem. Sci.*, 2012, **3**, 3175; (*b*) K. Cai, J. Xie and D. Zhao, *J. Am. Chem. Soc.*, 2014, **136**, 28; (*c*) K. Cai, J. Xie, X. Yang and D. Zhao, *Org. Lett.*, 2014, **16**, 1852.

10 (*a*) C. Roger and F. Würthner, *J. Org. Chem.*, 2007, **72**, 8070; (*b*) J. Misek, A. Jentzsch, S. Sakurai, D. Emery, J. Mareda and S. Matile, *Angew. Chem., Int. Ed.*, 2010, **49**, 7680; (*c*) C. Li, C. Xiao, Y. Li and Z. Wang, *Org. Lett.*, 2013, **15**, 682; (*d*) S. Suraru, C. Burschka and F. Würthner, *J. Org. Chem.*, 2014, **79**, 128; (*e*) S. Suraru and F. Würthner, *Angew. Chem., Int. Ed.*, 2014, **53**, 7428.

11 (*a*) M. J. Lin, B. Fimmel, K. Radacki and F. Würthner, *Angew. Chem., Int. Ed.*, 2011, **50**, 10847; (*b*) X. Fang, M. D. Guo, L. J. Weng, Y. Chen and M. J. Lin, *Dyes Pigm.*, 2015, **113**, 251.

12 S. Suraru and F. Würthner, *J. Org. Chem.*, 2013, **78**, 5227.

13 C. Tönshoff and H. F. Bettinger, *Angew. Chem., Int. Ed.*, 2010, **49**, 4125.

14 Y. Yamaguchi, K. Ogawa, K. Nakayama, Y. Ohba and H. Katagiril, *J. Am. Chem. Soc.*, 2013, **135**, 19095.

15 H. Usta, C. Risko, Z. Wang, H. Huang, M. K. Deliomeroglu, A. Zhu-khovitskiy, A. Facchetti and T. J. Marks, *J. Am. Chem. Soc.*, 2009, **131**, 5586.